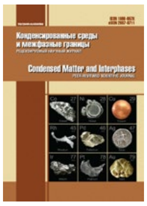

ISSN 1606-867X (Print)
ISSN 2687-0711 (Online)
Condensed Matter and Interphases
Kondensirovannye Sredy i Mezhfaznye Granitsy
https://journals.vsu.ru/kcmf/

Original articles

Research article
https://doi.org/10.17308/kcmf.2025.27/13296

Redox sorption of oxygen by Pd- and Cu-containing nanocomposites in the over-limiting current mode of electrochemical polarization

D. D. Vakhnin[1], T. E. Fertikova[2], N. A. Zheltoukhova[1], T. A. Kravchenko[1]✉, O. A. Kozaderov[1]

[1]Voronezh State University,
1 Universitetskaya pl., Voronezh 394018, Russian Federation

[2]Voronezh State Medical University named after N. N. Burdenko,
12 Studencheskaya st., Voronezh 394036, Russian Federation

Abstract

Objectives: Palladium- and copper-containing nanocomposites have been synthesized with different capacities for a metal component chemically deposited in a macroporous sulfocation exchange matrix.

Experimental: It has been revealed that in the over-limiting mode of electrochemical polarization, the reduction of oxygen dissolved in water on a palladium-containing nanocomposite proceeds by a catalytic mechanism. In addition to the targeted O_2 cathodic reduction process, adsorbed hydrogen is formed, which reacts catalytically with oxygen, which contributes to an additional decrease in O_2 concentration. It was found that in the over-limiting polarization mode of the Pd-containing nanocomposite, the oxygen concentration decreases significantly compared to the limiting mode.

Conclusions: The specific amount of absorbed oxygen increases with a decrease in the content of the deposited metal, which is associated with the high adsorption capacity of atomic hydrogen by weakly associated palladium nanoparticles. When using copper instead of palladium, the effectiveness of water deoxygenation decreases.

Keywords: Nanocomposite metal-ion exchange materials, Redox sorption, Deoxygenation of water

Funding: The study received financial support from the Ministry of Science and Higher Education of the Russian Federation within the framework of State Contract with universities regarding scientific research in 2025–2027, project No. FZGU-2025-0001.

For citation: Vakhnin D. D., Fertikova T. E., Zheltouhova N. A., Kravchenko T. A., Kozaderov O. A. Redox sorption of oxygen by Pd- and Cu-containing nanocomposites in the over-limiting current mode of electrochemical polarization. *Condensed Matter and Interphases*. 2025;27(4): 581–591. https://doi.org/10.17308/kcmf.2025.27/13296

Для цитирования: Вахнин Д. Д., Фертикова Т. Е., Желтоухова Н. А., Кравченко Т. А., Козадеров О. А. Редокс-сорбция кислорода Pd- и Cu-содержащими нанокомпозитами в сверхпредельном токовом режиме электрохимической поляризации. *Конденсированные среды и межфазные границы*. 2025;27(4): 581–591. https://doi.org/10.17308/kcmf.2025.27/13296

✉ Tamara A. Kravchenko, e-mail: krav280937@yandex.ru

1. Introduction

Modern physical chemistry pays special attention to systems containing nanometer-sized particles, since such systems have a huge specific surface area and, as a result, high excess energy, contributing to the intensification of industrially significant chemical or electrochemical processes. However, an unambiguous relationship between the reaction rate, size, and nature of the particles has not yet been established due to the simultaneous manifestation of a number of specific adsorption, structural, and percolation effects.

Special attention is paid to metal-ion exchanger nanocomposite materials, primarily because of their higher stability compared to single nanoparticles [1-5], as well as unique physical, chemical, and biological properties that arise due to the presence of particles smaller than one hundred nanometers in the composite material. The introduction of metal into the pores and on the surface of the ion exchanger matrix, which is a product of polymerization or polycondensation of unsaturated organic compounds, is ensured by the presence of acidic ($-SO_3H$, -COOH, -OH, $-PO_3H_2$, etc.) or basic ($-N(CH_3)_3$, $-NH_3$, $=NH_2$, etc.) functional groups in its structure. The metal can be embedded in an ion exchanger in the form of metal particles (usually nanometer-sized) or enter its matrix as oxides and poorly soluble hydroxides. The resulting hybrid nanostructures include reaction spaces and particles of composite components of the order of nanometers in size. By varying the polymer matrix material and the synthesis method, it is possible to obtain a nanocomposite with the necessary controlled structural properties. The pore volume of the matrix sets limits on the size of nanoparticle agglomerates, while the porous space depends on the degree of polymer crosslinking. In principle, there can be several nanoparticles in each individual pore. The minimum critical size of the nucleus depends on the initial concentration of atoms in the pore and the potential energy barrier of nucleation reduced due to the effect of the pore walls [6].

The particle size has a significant effect on the physicochemical characteristics of nanocomposites. An increase in the dispersion of the particles contained in them not only leads to a significant increase in the specific surface area, but also provides a dimensional effect of the first kind, which consists in the dependence of chemical and catalytic activity on the size of the cluster of nanoparticles. In addition, an energy dependence on the size of nanoparticles often occurs, and structural changes on the surface of nanoclusters additionally occur (changes in curvature, the appearance of crystallographic defects on the surface) [7-10]. The ambiguity of the role of the dimensional effect in the kinetics of electrochemical processes was revealed, for example, in [11] when studying the reaction of oxygen electroconduction on electrodes with platinum deposited on carbon. It turned out that in the methanol-containing electrolyte, the mass activity of the catalyst continuously increased with a decrease in the size of platinum nanoparticles from 4.6 to 2.3 nm. However, in an electrolyte without methanol, the activity of the same catalysts did not depend on the size of metal nanoparticles with a diameter of less than 3.5 nm.

The particle size is a thermodynamic variable that characterizes its state along with other system parameters [12]. The nanostructures have a higher surface energy by orders of magnitude than that of the medium and low-dispersed phases. As the particle size decreases, the ratio of the fractions of the surface and intraphase regions increases. If, for infinitely long phases, the internal energy, entropy, or volume at constant pressure and temperature depend linearly on the mass and amount of matter, then for the surface area of dispersed particles S, this dependence will be a power law:

$$S \approx n^{2/3}, \tag{1}$$

where n is the number of moles of the substance. As a result, none of the thermodynamic functions is linearly dependent on the mass. At the same time, the chemical parameters of particles of various sizes differ significantly from the specific values. If a crystal has a volume V and a surface S constructed of various faces with areas S_i and edges of length l_k, then the Gibbs energy is:

$$G = g^V V + \sum \sigma_i S_i + \sum \tau_k l_k, \tag{2}$$

where g^V is the specific G value per unit volume, σ_i is the specific G value per 1 cm^2 for i-faces, τ_k is the same value per unit length of k-edges.

In the special case of a spherical nanoparticle with radius r, the excess chemical potential relative to the continuum potential is determined by the Gibbs-Thomson (Kelvin) equation:

$$\Delta\mu_r = \mu_r - \mu_\infty = \frac{\sigma V_m g}{r}, \tag{3}$$

where σ is the reversible work of a surface unit (for a liquid, this is surface tension); V_m is the molar volume of a substance, g is the geometric factor ($g = 2$ for spherical particles).

A secondary dimensional effect occurs at a certain size of nanoparticles, when there is a fluctuating redistribution of charges between particle ensembles, which can lead to an increase in the catalytic activity of the material [13]. However, a decrease in particle size does not entail such an increase under all conditions. In [14], the extreme dependence of the catalytic activity of platinum on a carbon substrate on the size of nanoparticles in the oxygen reduction reaction was shown. To explain this phenomenon, the concept of surface effects was formulated, which assumes that as the particle size decreases, the surface energy increases and changes occur in the electronic structure of the surface. This can lead to a change in the activity of the catalytic surface, for example, to a change in the donor-acceptor properties of the surface and the electronic structure of the metal on the surface. However, the dimensional effects can be compensated by other factors, such as changes in the shape and structure of the particles, the composition of the starting materials, the degree of particle dispersion on the substrate, and others. In addition, the catalytic activity may change as the reaction conditions change. Obviously, studying the size effects and other factors affecting the catalytic activity of nanoparticles is important for developing effective catalysts for various reactions.

Nanocomposites are characterized by the manifestation of percolation effects, that is, an abrupt change in the physico-chemical characteristics with a linear change in the amount of one of the constituent components. Thus, in [15], an increase in the mass transfer rate on a complex metal polymer doped with gold was revealed at the threshold of electron conduction percolation due to a decrease in the interparticle distance. After 5 cycles of chemical deposition of silver nanoparticles onto the MF-4SK membrane, the ohmic resistance of the modified membrane dropped sharply [16]. In the case of the CU-23 sulfocation exchanger, the oxygen reduction rate increased sharply with a copper content of ~5 meq/cm^3 [17]. The authors explain the drop by the transition from single nanoparticles to their unified system with generalized electrons. Ionic conductivity is similarly susceptible to percolation effects [18], which is expressed in an increase in sorption of mobile ions due to a large surface defect.

The most common and significant factor in the applied aspect reaction is oxygen electroreduction, and therefore it is being actively investigated. Oxygen reduction is widely used in fuel cells [19] and electrocatalysis [20]. Oxygen acts as a depolarizer in metal corrosion [21]. Deep deoxygenation of water is also required for the needs of microelectronics, where ultrapure water is used at the stage of flushing silicon wafers in the manufacture of integrated circuits. To prevent the formation of an oxide layer on the plate surface, the O_2 content level should not exceed 1 μg/l [22]. Thus, the oxygen reduction reaction undoubtedly plays a huge role in many industrially significant processes. The problem of organizing a potable water supply for the populations of large cities is caused, among other things, by the presence of dissolved oxygen in the water. Being a strong corrosive agent and interacting with pipeline materials, O_2 causes a change in their composition and structure, which leads to a deterioration in the quality of potable water supplied to the population and a violation of hygienic standards [23, 24]. It should be noted that at present, official data from the Federal Service for Surveillance on Consumer Rights Protection and Human Wellbeing indicate an improvement in the quality of drinking water in water pipes [25, 26]. Within the territory of the Russian Federation, there has been a decrease in the proportion of water samples that do not meet hygienic standards for sanitary and chemical indicators from 17.2 to 15.5%, and for microbiological ones from 3.6 to 1.9% in 2022 compared with 2013. According to microbiological indicators, the proportion of samples that did not meet the requirements was at the level of 2021 and amounted to 0.9%. However, this information is based on the results of a study of water before entering the distribution network, which does not preclude a decrease in its quality as a result of passing through pipelines.

Hybrid catalytic nanocomposite systems in which oxygen reduction is organized by both the chemical interaction of dissolved O_2 with gaseous hydrogen [3, 27, 28] and its electrochemical reduction, when both processes occur on metal nanoparticles stabilized in an ion exchange matrix [29-31], seem to be the most promising for deep deoxygenation of water. Obviously, depending on the nature of the metallic and ion-exchange components of the nanocomposite, as well as on the conditions of electrochemical polarization, the contributions to the overall process of each of the partial reactions will be different. For comparison with a copper-containing nanocomposite, a palladium-containing nanocomposite was studied, on which, as is known, the catalytic reaction between adsorbed hydrogen and oxygen proceeds best. At the same time, the issues of both the mechanism of redox sorption of molecular oxygen from water in over-limiting polarization regimes and the contributions of partial stages of the process remain insufficiently resolved.

The purpose of the work was to study the process of redox oxygen sorption on palladium- and more affordable copper-containing ion-exchange nanocomposites in the mode of over-limiting polarization.

2. Experimental

A macroporous strongly acidic ion exchange matrix CU-23 15/100 was used for the synthesis of nanocomposites (NC) (Table 1). It is characterized by the presence of sulfogroups on the surface and in the volume of the polymer and the predominance of macropores with a fairly wide size distribution.

The polymer chain of the ion exchange matrix has the following form:

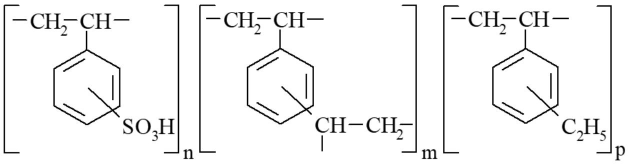

where n, m, p are the number of components in the polymer. The selected ion-exchange porous matrix has sufficient mechanical strength, is resistant to acid-base influences, and does not undergo thermal decomposition over a sufficiently wide temperature range.

The chemical deposition of metal into the ion exchange matrix was preceded by its preliminary preparation [33]. The ion exchanger was placed in 2 M NaCl for a day, then its acid-base conditioning was carried out, consisting in sequential dynamic passage through a column for the synthesis of HCl and NaOH solutions with a solution:ion exchanger volume ratio of 3:1 with decreasing concentration (1.0 M; 0.5 M; 0.25 M). After each acid/alkali pass, the ion exchanger was washed with a large amount of distilled water. The ANION-4100 ionomer (Infraspak-Analyte, Russia) recorded the alignment of pH of the solution at the outlet of the column and pH of distilled water.

The synthesis of the nanocomposite consisted of two stages: saturation of the matrix with metal ions and their subsequent chemical reduction. To saturate the cation exchanger with copper (II) ions, a 6% solution of copper (II) sulfate in water was passed through the bulk layer of the ion exchanger at the rate of 10 volumes of solution per 1 volume of resin at a volumetric rate of $5 \cdot 10^{-4}$ m^3/h. During this stage, the ion exchange of metal cations and hydrogen of the ionogenic centers of the sulfogroups of the ion exchanger took place. Then, the non-exchangeably sorbed electrolyte was washed out of the cation exchanger with distilled water deoxygenated with argon. Chemical reduction of the metal was carried out with 0.35 M sodium dithionite $Na_2S_2O_4$ solution in 0.63 M NaOH in a volume ratio of reducing agent solution/ion exchanger equal to 10:1. Then the copper-containing nanocomposite was washed from the reducing agent, neutralizing the alkali with an hydrochloric acid solution

Table 1. Basic physico-chemical characteristics of an ion exchanger [32]

The cation exchanger	CU-23 15/100
Polymer base	Stitched polystyrene
Ion exchange (redox) capacity of granular volume, meq/cm^3	1.25
Characteristic pore diameter, nm	10–100
Specific pore volume, cm^3/g	0.40–0.60
Diameter of granules, mm	0.40–1.25

followed by passing deoxygenated distilled water. If necessary, to convert the nanocomposite to the Na^+ form, a solution of sodium sulfate was passed through the synthesis column and washed with distilled water, deoxygenated by hour-long argon bubbling. The cycles of ion exchange saturation and reduction of the metal deposited in the ion exchange matrix were repeated several times until a nanocomposite with the required metal capacity was obtained.

In the case of palladium-containing nanocomposites, the saturation solution was a 6% palladium (II) chloride solution, which was passed from bottom to top in even cycles of palladium deposition and from top to bottom in odd cycles at a speed of 5 m/h. The amount of solution consumed was in a ratio of 5:1 to the volume of resin; the transmission time was 30–40 minutes. After washing with deoxygenated water, a solution of the reducing agent, sodium borohydride, was passed through in an alkaline medium at a rate of 5 m/h for an hour. Washing with distilled water was carried out from the top down at a rate of 10 m/h. The water volume to resin volume was 10:1, with a flow time of 1 hour. The synthesis of the palladium-containing composite was accompanied by a rapid release of gas.

To determine the redox capacity of NC for copper, a titrimetric method was used, for which 1 cm^3 of the test sample was placed in a heat-resistant glass in a water bath, and 10% nitric acid was sequentially added to it in 10 ml portions. The copper cations formed during dissolution passed into a solution, which was then transferred to a measuring flask until the entire metal of the composite dissolved, which was visually detected by the absence of a change in the color of the nitric acid solution. The resulting solution containing copper ions was brought to the mark in a measuring flask and the redox capacity was determined. The metal capacity was determined by transferring the entire metal sample into a 100 cm^3 solution using nitric acid. Then, an aliquot of 10 cm^3 was taken from the resulting solution, which was additionally diluted with 20 cm^3 of distilled water and treated with an ammonia buffer solution (20 g/l NH_4Cl + 100 cm^3 NH_3) until an alkaline medium was obtained and the solution acquired a blue color. The concentration of copper ions was determined by complexometric titration using 0.1 mol-eq/cm^3 of trilon B and murexide as an indicator before the color of the solution changed to purple.

Titrimetric determination of palladium in solution began with the preparation of an analyte – standard solutions of palladium and EDTA, a titrant – a standard solution of zinc, an indicator solution of “eriochrome black T”. Preparation of a standard palladium solution: 1.5 g of pure palladium was dissolved in several milliliters of aqua regia. Nitrogen oxides were removed by evaporation with hydrochloric acid. The dry residue was dissolved in 0.2 M hydrochloric acid and adjusted with the same solution to a volume of 500 ml. Preparation of a standard zinc solution: 1.8 g of zinc oxide was dried at 100 °C for 2 hours, dissolved in a minimum volume of nitric acid (1:1) and brought to a volume of 1 liter. Preparation of a standard EDTA solution: 5.5 g of sodium salt of EDTA was dissolved in a liter of distilled water. The titer of the solution was determined by complexometric titration with a standard zinc solution and “eriochrome black T” as an indicator. Preparation of the indicator solution: 0.1 g of “eriochrome black T” was dissolved in 50 ml of distilled water, to which several drops of 1 M solution of caustic potassium were added. The course of the analysis: a small excess of the standard EDTA solution was added to the standard palladium (II) chloride solution. By adding 0.1 M solution of caustic potassium, the pH was set to 10±1. 5 drops of “eriochrome black T” solution were added and titrated with a standard zinc solution until the equivalence point, which was determined by the color change from blue or green to bright pink.

The redox capacity of the deposited metal $\varepsilon_{\mathrm{Me}^0}$, mol-eq/cm^3 in the sample was calculated by the formula:

$$\varepsilon_{\mathrm{Me}^0} = \frac{C_{\mathrm{T}} V_{\mathrm{T}} V}{V_{\mathrm{NC}} V_{\mathrm{Al}}}, \tag{4}$$

where C_{T} is the titrant concentration, mol-eq/cm^3; V_{T}, V, V_{NC}, V_{Al} are the volumes of the titrant, the total solution, the sample of NC granules taken for analysis, and the aliquot taken for titration, respectively. All volumes are taken in the same units, for example, cm^3.

The approach described in [29] was used to select the value of the polarizing current. It is based on the concepts of external diffusion oxygen transport and the density of the limiting oxygen diffusion current. The maximum allowable current for the entire granular layer, i.e. the limiting current of I_{lim}, is equal to

$$\frac{I_{\text{lim}}}{I_{\text{com}}} = \frac{Al}{1+Al}, \tag{5}$$

where I_{com} is the current required to reduce all oxygen entering the column:

$$I_{\text{com}} = nFSuc_0, \tag{6}$$

S is the cross-sectional area of the granular layer (1.2 cm); u is the flow rate (0.23 cm/s); l is the height of the granular layer (1 cm), and c_0 is the oxygen concentration in the water at the entrance to the granular layer (7.7 mg/l).

The value of the constant A is found by the formula:

$$A = \frac{3\chi i_{\text{lim}}(0)}{nFuR_0c_0}, \tag{7}$$

where χ is the coefficient of column filling with sorbent, $i_{\text{lim}}(0)$ is the density of the limiting diffusion current on the surface of the NC granule, R_0 is the radius of the NC granule. The calculated parameters are shown in Table 2.

Table 2. Calculated parameters of the experiment

$i_{\text{lim}}(0)$, A/m^2 [29]	A, cm^{-1}	I_{com}, mA	I_{lim}, mA
1.03	0.24	25.6	5.0

Granular nanocomposite materials were loaded into the cathode compartment of a sorption-membrane electrochemical cell, the scheme of which is shown in Fig. 1. The three-chamber electrolyzer contains a cathode compartment separated from the two anode membranes by MC-40. The bulk cathode was a thin copper wire surrounded by a layer of NC. The anodes were made of platinum wire twisted into a spiral. An appropriate ion exchanger was loaded into the anode chambers, which did not contain any deposited metal particles inside.

A MC-40 cation exchange membrane was used to ensure proton transfer from the anode to the cathode. The height of the thin granular nanocomposite layer was $l = 1$ cm, and the cross-sectional area of the nanocomposite layer was $S = 1.2$ cm^2. Water flowed through the electrolyzer at a rate of u = 0.23 cm/s. An AKIP-1111 (Russia) was used as an external current source. To measure the concentration of the oxidizer, an AKPM-01 oxygen meter (Alfa-Bassens LLC, Russia) was used, protected from external electromagnetic radiation by a metal mesh screen. The oxygen input concentration was kept constant by continuously supplying atmospheric air to a container with distilled water before entering the reactor. After the thin granular layer of the nanocomposite, a filter was installed that performed the functions of sorption and membrane filtration. The value of water pH at the outlet of the electrolyzer was measured using an ionomer ANION-4100 manufactured by "Infraspak-Analyt", Russia.

3. Results and discussion

As a result of the procedures of saturation of the ion exchanger with counterions of the deposited metal, their subsequent reduction with an alkaline solution of a reducing agent and conversion to the initial ionic form, metal-ion exchange nanocomposites with different capacities for the metal component were obtained. Chemical precipitation of copper into a macroporous sulfocation exchanger with sodium dithionite in an alkaline medium occurred according to the scheme:

$$2\text{R-SO}_3^-\text{H}^+ + \text{Cu}^{2+} \rightleftarrows (\text{R-SO}_3^-)_2\text{Cu}^{2+} + 2\text{H}^+ \tag{8}$$

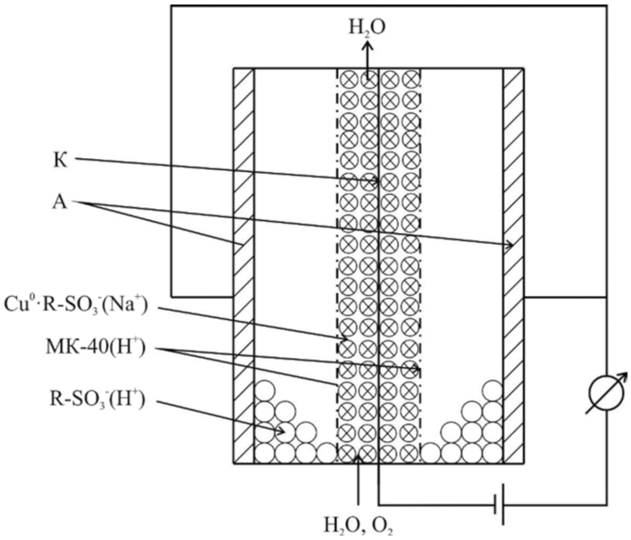

Fig. 1. Scheme of a three-chamber sorption-membrane electrolyzer for deoxygenation of flowing water. C is a copper wire current supply, $\text{Cu}^0 \cdot \text{R-SO}_3^-$ is a bulk layer of nanocomposite; A is platinum wire anodes, R-SO_3^- are bulk layers of a sulfocation exchanger; MC-40 (H$^+$) is a cation exchange membrane

$$(\text{R-SO}_3^-)_2\text{Cu}^{2+} + \text{Na}_2\text{S}_2\text{O}_4 + 4\text{NaOH} \rightarrow \rightarrow \left[\text{R}-\text{SO}_3^-\text{Na}^+\right]_2 \cdot \text{Cu}^0 + 2\text{Na}_2\text{SO}_3 + 2\text{H}_2\text{O} \quad (9)$$

$$\left[\text{R}-\text{SO}_3^-\text{Na}^+\right]_2 \cdot \text{Cu}^0 + 2\text{H}^+ \rightarrow \rightarrow \left[\text{R}-\text{SO}_3^-\text{H}^+\right]_2 \cdot \text{Cu}^0 + 2\text{Na}^+ \quad (10)$$

The chemical precipitation of palladium in a sulfocation exchanger with sodium borohydride in an alkaline medium occurred according to the scheme:

$$2\text{R-SO}_3^-\text{H}^+ + \text{PdCl}_2 \rightarrow \left(\text{R-SO}_3^-\right)_2\text{Pd}^{2+} + 2\text{HCl} \quad (11)$$

$$(\text{R}-\text{SO}_3^-)_2\text{Pd}^{2+} + 2\text{NaBH}_4 + 6\text{H}_2\text{O} \rightarrow \rightarrow \left[\text{R}-\text{SO}_3^-\text{Na}^+\right]_2 \cdot \text{Pd}^0 + 2\text{B(OH)}_3 + 7\text{H}_2 \quad (12)$$

The values of the metal capacity of the obtained nanocomposites are given in Table 3.

The current I = 50 mA was selected for polarization in the over-limiting mode, i.e. the excess of the maximum current was I/I_{lim} was 10. The current was turned on for 4 hours after the oxygen concentration was established for an hour, and after 5 hours of the experiment, the current was turned off. Oxygen concentration measurements were continued for another 5 hours. During this time, the oxygen concentration in the water at the outlet of the granular layer of NC reached the initial value at the inlet.

The amount of dissolved oxygen removed from the water (moles) was calculated based on the difference in the amount of oxygen dissolved in the water at the entrance to the granular layer of the nanocomposite and at the exit:

$$Q(\text{O}_2) = (c_0 - \bar{c})\frac{u \cdot t}{\text{M}_r(\text{O}_2)}, \quad (13)$$

where c_0 is the concentration of oxygen dissolved in water at the inlet (mg/l), $\bar{c}$ is the average value of the residual (output) concentration in three duplicate experiments, t is the experiment time, u is the volume flux of water (0.8 l/h), M_r (O_2) is the molar mass of oxygen.

The calculation results are presented in Table 3. It can be seen that during the deoxygenation of water in the selected over-limiting mode of electrochemical polarization, a significant amount of gas was released. Oxygen dissolved in water is removed in various ways: 1) by direct electroreduction, 2) by catalytic interaction with electrochemically obtained adsorbed atomic hydrogen or chemical oxidation of electrochemically reduced active metal nanoparticles from oxides, and 3) by physical removal with released hydrogen. At the same time, all these stages took place under the influence of cathodic polarization. After the current was turned off, the oxygen concentration gradually equalized to the initial level due to the finite mixing time of the running water in the measuring vessel.

Oxygen can electrochemically interact with hydrogen ions, which leads to the basic reaction with the formation of water. At pH < 7, which is true for the hydrogen ionic form of the

Table 3. Metal capacity, volume of released gas, and amount of oxygen removed from water for $\text{Pd}^0\cdot$CU-23 (H^+) and $\text{Cu}^0\cdot$CU-23 (H^+) nanocomposites. Experimental conditions: granular layer height l = 1 cm, water flow rate u = 0.23 cm/s, I = 50 mA, I/I_{lim} = 10

Nanocomposites, number of metal deposition cycles	$\varepsilon_{\text{Mr}^0}$, mmole-eq/cm^3 (mmol/cm^3)	V(H_2,O_2), cm^3	Q (H_2,O_2) n the gas mixture, mmol	$\sum Q(\text{O}_2)$, removed from water, mmol	$Q(\text{O}_2)$, emoved under current (stage 2), mmol	$Q(\text{O}_2)$, removed without current (stage 3), mmol
$\text{Pd}^0\cdot$CU-23 (H^+), 1	0.76±0.23 (0.38±0.12)	22.3±1.0	0.91	0.72	0.49	0.23
$\text{Pd}^0\cdot$CU-23 (H^+), 3	3.22±0.23 (1.61±0.12)	27.7±2.0	1.13	0.78	0.50	0.28
$\text{Pd}^0\cdot$CU-23 (H+), 5	5.02±0.14 (2.51±0.07)	30.0±2.0	1.23	0.74	0.44	0.30
$\text{Cu}^0\cdot$CU-23 (H^+), 10	9.68±0.07 (4.84±0.04)	58.3±3.0	2.39	0.79	0.44	0.35
CU-23 (H^+), 0	0	45.0±1.2	1.84	0.44	0.41	0.03

nanocomposite, the oxygen reduction reaction can be represented as [34]:

$$O_2 + 4H^+ + 4e^- \rightarrow 2H_2O \;\; (E^0 = 1.23\text{ V}), \qquad (14)$$

and in a neutral and alkaline environment according to the equation:

$$O_2 + 2H_2O + 4e^- \rightarrow 4OH^- \;\; (E^0 = 0.40\text{ V}). \qquad (15)$$

During the over-limiting polarization on the palladium surface, the formation of adsorbed hydrogen became possible, due to the catalytic activity of which the oxygen reduction reaction with the formation of water was carried out [27]:

$$2H^+ + 2e^- \xrightarrow{I} 2H_{ads} \qquad (16)$$

$$O_2 + 4H_{ads} \xrightarrow{Pd} 2H_2O \qquad (17)$$

On copper-containing nanocomposites, due to interaction with oxygen, the formation of copper oxides is possible: Cu_2O and CuO. The chemical activity of the nanocomposite is kept due to the electroreduction of copper from oxides [29]:

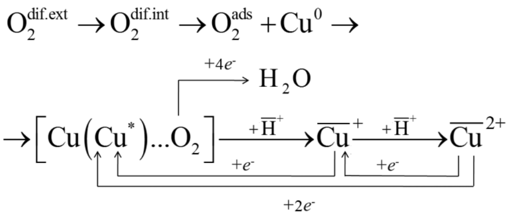

$$O_2^{\text{dif.ext}} \rightarrow O_2^{\text{dif.int}} \rightarrow O_2^{\text{ads}} + Cu^0 \rightarrow$$

$$\xrightarrow{+4e^-} H_2O$$

$$\rightarrow \left[Cu\left(Cu^*\right)...O_2\right] \xrightarrow[+e^-]{+\overline{H}^+} \overline{Cu}^+ \xrightarrow[+e^-]{+\overline{H}^+} \overline{Cu}^{2+}$$

$$+2e^-$$

Here $\overline{H}^+$, $\overline{Cu}^+$, $\overline{Cu}^{2+}$ are the counterions.

It is possible to physically displace oxygen dissolved in water with an inert gas, which can be released by molecular hydrogen.

The experiment can be divided into 3 stages. The first lasting 1 hour is the establishment of stationarity, the second (2-5 hours) is the time of electrochemical reactions, and the third (5-10 hours) is catalytic for palladium-containing NC, or chemical for copper–containing NC oxygen reduction. Fig. 2 shows a decrease in the relative oxygen concentration to ~0.3 at Pd^0·CU-23 (H^+), which is associated with the high ability of palladium to hydrogenate and an active catalytic reaction between oxygen and molecular hydrogen on the Pd surface. During the polarization of the Pd^0·CU-23 (H^+) nanocomposite, the pH value of water was in the range of 6.4–7.0. Compared with palladium nanocomposites for Cu^0·CU-23 (H^+), the concentration of C/C_0 oxygen dissolved in water decreased to ~0.4 (Fig. 3). During the experiment, the pH value increased from 6.5 to 6.7.

The current efficiency for molecular hydrogen evolution and the efficiency of oxygen removal are shown in Table 4. They show the ratio of the contributions of electrochemical processes. A dimensionless efficiency coefficient of nanocomposites for water deoxygenation has been introduced:

$$f_{\text{deox}} = \frac{\sum Q(O_2)}{\nu \varepsilon_{Me^0} V_{NC}}, \qquad (19)$$

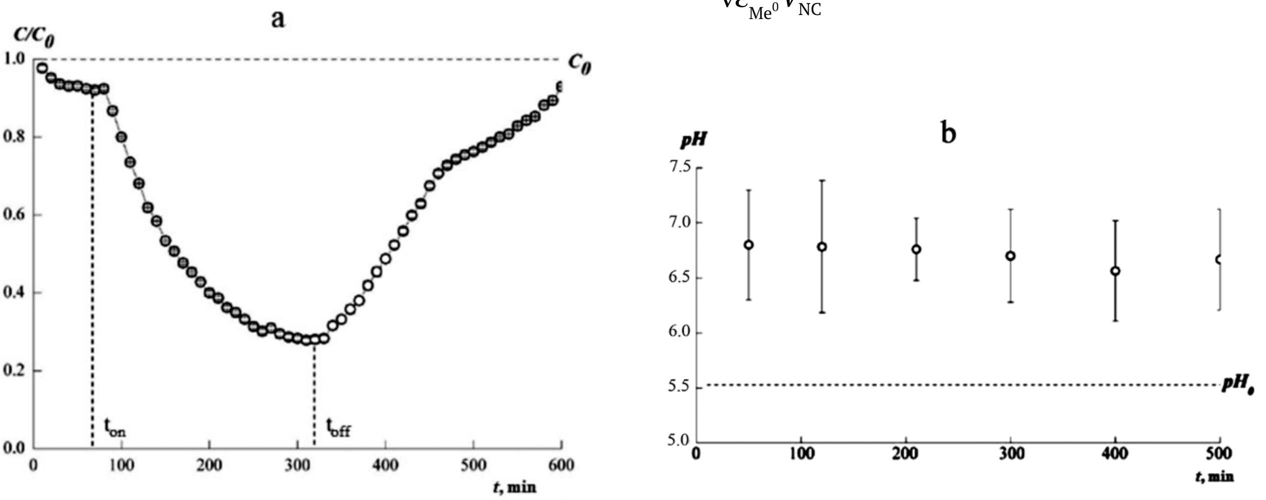

Fig. 2. Relative concentration C/C_0 of dissolved oxygen (a), and pH of water (b) at the outlet of a thin granular layer of the Pd^0·CU-23(H^+) nanocomposite in the over-limiting polarization mode. Experimental conditions: the height of the granular layer is l = 1 cm, 1 cycle of metal deposition. C_0 is the initial oxygen concentration (7.9 mg/l), pH_0 is the hydrogen index of the source water. Ionic forms in the cathode and anode chambers of CU-23(H^+), I = 50 mA, I/I_{lim} = 10, limiting current I_{lim} =5.0 mA, t_{on}, t_{off} are the times of switching on and off the current, respectively

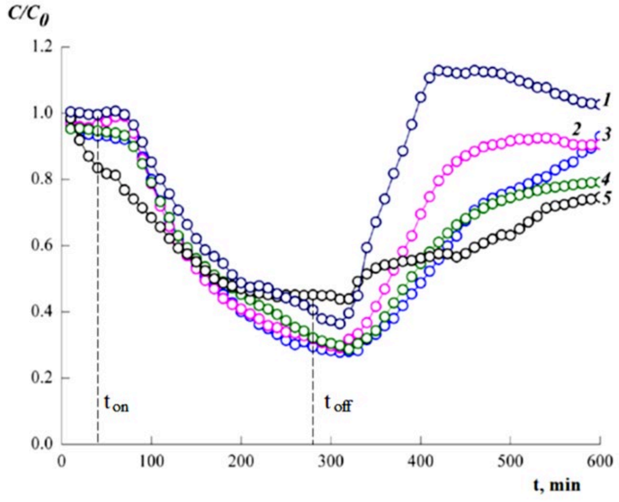

Fig. 3. Relative concentration C/C_0 of dissolved oxygen in water at the outlet of a thin granular layer of nanocomposites. Experimental conditions: granular layer height l = 1 cm, water flow velocity u = 0.23 cm/s, I = 50 mA, I/I_{lim} = 10, I_{lim} =5.0 mA. C_0 is the initial oxygen concentration (7.4-8.0 mg/l), t_{on}, t_{off} are the times of switching on and off the current, respectively. Curves: 1 – CU-23 (H^+); 2 – Pd^0·CU-23 (H^+), one deposition cycle; 3 – Pd^0·CU-23 (H^+), three deposition cycles; 4 – Pd^0·CU-23 (H^+), five deposition cycles; 5 – Cu^0·CU-23 (H^+), ten deposition cycles

in which the amount of oxygen removed (mmole) is normalized to the stoichiometric coefficient of the metal (Pd, Cu) in reaction with oxygen (2), the metal capacity (mmol/cm^3) and the volume of the granular layer of the V_{NC} nanocomposite. The efficiency coefficient of water deoxygenation decreased significantly with an increase in the number of plantings of deposited palladium (Table 4).

Table 4. Oxygen and hydrogen current efficiency, and nanocomposites efficiency coefficient for water deoxygenation. The polarizing current I = 50 mA, I/I_{lim} = 10

Nanocomposites, number of metal deposition cycles	$\eta_T(H_2)$, %	$\eta_T(O_2)$, %	f_{deox}, %
Pd^0·CU-23 (H+), 1	58.0	42.0	78.9
Pd^0·CU-23 (H+), 3	63.0	37.0	20.2
Pd^0·CU-23 (H+), 5	67.7	32.3	12.3
Cu^0·CU-23 (H+), 10	73.0	27.0	6.8
CU-23 (H+), 0	70.0	30.5	–

Thus, an increase in the amount of palladium embedded in NC does not increase the efficiency of the redox sorption process. Only the amount of released hydrogen gas increases. The specific amount of reduced oxygen decreases steadily with increasing palladium capacity. Based on the corresponding dependencies in Fig. 4, it can be concluded that in order to intensify the process of water deoxygenation, it is not necessary to increase the amount of metal in the nanocomposite. On the contrary, an increase in the specific content of reduced oxygen will occur with a small number of metal nanoparticles that are not combined into aggregates, and therefore their surfaces are characterized by the greatest access for adsorption.

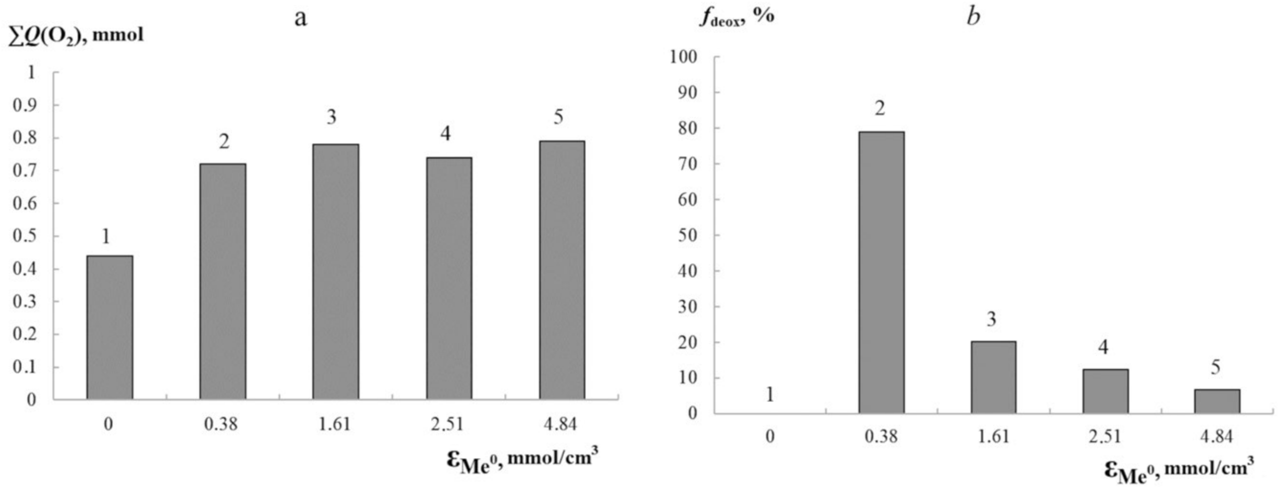

Fig. 4. Histograms of the distribution of the amount of oxygen removed ∑Q(O_2) (a) and the efficiency coefficient of nanocomposites for water deoxygenation f_{deox} on the metal capacity (b): 1 – CU-23(H^+), 2-4 – Pd^0·CU-23 (H^+); 5 – Cu^0·CU-23 (H^+). Experimental conditions: granular layer height l = 1 cm, 1, 3, 5, and 10 cycles of metal deposition, water flow rate u = 0.23 cm/s, polarizing current I = 50 mA, I/I_{lim} = 10, I_{lim} = 5 mA

4. Conclusions

Palladium- and copper-containing nanocomposites with different capacities for the metal component deposited in a macroporous sulfocation exchange matrix have been synthesized.

In the over-limiting polarization mode on paladium-containing nanocomposites, the concentration of oxygen dissolved in water passing through the granular layer decreases significantly compared to the limiting mode. In addition to the electroreduction of oxygen, adsorbed hydrogen is formed, which enters into a catalytic reaction with dissolved oxygen, as well as the physical displacement of oxygen by gaseous hydrogen, which leads to an additional decrease in oxygen concentration.

The specific amount of absorbed oxygen increases with a decrease in the content of deposited metal, which is associated with a decrease in the size of nanoparticle aggregates. With some reduction in efficiency, it is possible to use copper instead of palladium.

Contribution of the authors

The authors contributed equally to this article.

Conflict of interests

The author declares that they have no known competing financial interests or personal relationships that could have appeared to influence the work reported in this paper.

References

1. *Nanoparticle Technology Handbook. Masuo Hosokawa, Kiyoshi Nogi, … Toyokazu Yokoyama* (eds.). Elsevier Science; 2008. https://doi.org/10.1016/B978-0-444-53122-3.X5001-6

2. *Nanocomposites: Synthesis, Characterization and Applications* X. Wang (ed.). New York: Nova Sc. Publ.; 2013. 422 p.

3. Volkov V. V., Kravchenko T. A., Roldughin V. I. Metal nanoparticles in catalytic polymer membranes and ion-exchange systems for advanced purification of water from molecular oxygen. *Russian Chemical Reviews*. 2013;82(5): 465–482. https://doi.org/10.1070/rc2013v082n05abeh004325

4. Povolotskaya A. V., Povolotskiy A. V., Manshina A. A. Hybrid nanostructures: synthesis, morphology and functional properties. *Russian Chemical Reviews*. 2015;84(6): 579–600. https://doi.org/10.1070/RCR4487

5. Lateef A., Nazzir R. Metal Nanocomposites: Synthesis, Characterization and their Applications. In book: *Science and applications of Tailored Nanostructures*. *Ch. 12.* Paolo Di Sia (ed.). Publisher: One central press; 2017. p. 239–256. Available at: https://www.researchgate.net/publication/313634485

6. Capek I. *Nanocomposite structures and dispersions*. Amsterdam: Elsevier; 2006. 301 p.

7. Proch S., Wirth M., White H. S., Anderson S. L. Strong effects of cluster size and air exposure on oxygen reduction and carbon oxidation electrocatalysis by size-selected Ptn (n ⩽ 11) on glassy carbon electrodes. *Journal of the American Chemical Society*. 2013;135: 3073–3086. https://doi.org/10.1021/ja309868z

8. Nesselberger M., Roefzaad M., Hamou R F., … Arenz M. The effect of particle proximity on the oxygen reduction rate of size-selected platinum clusters. Nature Materials. 2013;12: 919–924. https://doi.org/10.1038/nmat3712

9. *Nanoparticles and catalysis*. Astruc D. (ed.). Weinheim: Wiley-VCH Verlag GmbH & Co; 2008. 663 p.

10. Reske R., Mistry H., Behafarid F., Roldan Cuenya B., Strasser P. Particle size effects in the catalytic electroreduction of CO_2 on Cu nanoparticles. *Journal of the American Chemical Society*. 2014;136(19): 6978–6986. https://doi.org/10.1021/ja500328k

11. Maillard F., Martin M., Gloaguen F., Lйger J.-M. Oxygen electroreduction on carbon-supported platinum catalysts. Particle-size effect on the tolerance to methanol competition. *Electrochimica Acta*. 2002;47(21): 3431–3440. https://doi.org/10.1016/s0013-4686(02)00279-7

12. Poltorak O. M. *Lectures on chemical thermodynamics**. Moscow: Vysshaya shkola Publ.; 1971. 256 p. (in Russ.)

13. Rostovshchikova T. N., Smirnov V. V., Kozhevin V. M., Yavsin D. A., Gurevich S. A. Intercluster interactions in catalysis by nanosized particles*. *Nanotechnologies in Russia*. 2007;2(1-2): 47–60. (in Russ.). Available at: https://elibrary.ru/item.asp?id=9321693

14. Leontyev I. N., Belenov S. V., Guterman V. E., Haghi-Ashtiani P., Shaganov A. P., Dkhil B. Catalytic activity of carbon-supported Pt nanoelectrocatalysts. Why reducing the size of Pt nanoparticles is not always beneficial. The Journal of Physical Chemistry C. 2011;115(13): 5429–5434. https://doi.org/10.1021/jp1109477

15. Forster R. J., Keane L. Nanoparticle–metallopolymer assemblies: charge percolation and redox properties. *Journal of Electroanalytical Chemistry*. 2003;554-555: 345–354. https://doi.org/10.1016/S0022-0728(03)00258-4

16. Shel’deshov N. V., Mel’nikov S. S., Solov’eva T. T., … Zabolotskii V. I. The effect of silver ions and nanoparticles on the properties of ion-exchange materials. *Russian Journal of Electrochemistry*. 2011;47(2): 200–208. https://doi.org/10.1134/s1023193511020157

17. Chaika M. Yu., Kravchenko T. A., Polyanskii L. N., Krysanov V. A. Electroreduction of molecular oxygen on dispersed copper in an ion-exchange matrix. *Russian Journal of Electrochemistry*. 2008;44(11): 1244–1250. https://doi.org/10.1134/s1023193508110086

18. Yaroslavtsev A. B. Correlation between the properties of hybrid ion-exchange membranes and the nature and dimensions of dopant particles. *Nanotechnologies in Russia*. 2012;7(9–10): 437–451. https://doi.org/10.1134/s1995078012050175

19. Gattrell M., MacDougall B. Reaction mechanisms of the O_2 reduction/evolution reaction. In book: Handbook of Fuel Cells – Fundamentals, Technology and Applications.

Vol. 2. Part 5. Electrocatalysis. John Wiley & Sons; 2003. p. 443-464. https://doi.org/10.1002/9780470974001.f205034

20. *PEM Fuel Cell Electrocatalysts and Catalyst Layers. Fundamentals and Applications.* J. Zhang (ed.). Springer; 2008. 1137 p.

21. Semenova I. V., Florianovich G. M., Khoroshilov A. V. *Corrosion and corrosion protection*. I. V. Semenova (ed.). Moscow: Fizmatlit Publ.; 2002. 336 p. (in Russ.)

22. Volkov V. V., Petrova I. V., Yaroslavtsev A. B., Tereshchenko G. F. Deep purification of water from dissolved oxygen for microelectronics, power plants and the food industry*. *Russian Membrane Society website*. (in Russ.). Available at: http://memtech.ru/index.php/ru/glavnaya/publications/200-udalenie-kisloroda-iz-vody

23. SanPiN 2.1.3684-21 *“Sanitary and epidemiological requirements for the maintenance of the territories of urban and rural settlements, water bodies, drinking water and drinking water supply, atmospheric air, soils, residential premises, operation of industrial and public premises, organization and implementation of sanitary and anti-epidemic (preventive) measures*.”* 66 p. (in Russ.)

24. SanPiN 1.2.3685-21 “*Hygienic standards and requirements for ensuring the safety and (or) harmlessness of environmental factors for humans*.”* 1143 p. (in Russ.)

25. On the state of sanitary and epidemiological well-being of the population in the Russian Federation in 2022. *State report**. Moscow: Federal Service for Surveillance on Consumer Rights Protection and Human Welfare, 2023. 368 p. (in Russ.)

26. Report *“On the state of sanitary and epidemiological well-being of the population in the Voronezh region in 2023*”*. Voronezh: Office of the Federal Service for Surveillance on Consumer Rights Protection and Human Wellbeing in the Voronezh Region, 2024. 199 p. (in Russ.)

27. Gurskii V. S., Kirpikov D. A., Kharitonova E. Yu., Tsapko Yu. V., Yasnev I. M. Catalytic deoxygenation of high-purity water using membrane electrode units. *Russian Journal of Applied Chemistry*. 2015;88(10): 1656–1660. https://doi.org/10.1134/s107042721510016x

28. Kirpikov D. A., Pykhteev O. Ju., Kharitonova E. Ju., Tsapko Ju. V., Chistjakov I. V., Gurskij V. S. *Device for electrochemical deoxygenationof highly pure water.* Patent RF, no. 2494974, 2012. Publ. 10.10.2013, bull. no. 28. 9 p. (in Russ.)

29. Kravchenko T. A., Zolotukhina E. V., Chaika M. Yu., Yaroslavtsev A. B. *Electrochemistry of metal-ion exchanger nanocomposites**. Moscow: Nauka Publ.; 2013. 363 p. (in Russ.)

30. Fertikova T. E., Fertikov S. V., Isaeva E. M., Krysanov V. A., Kravchenko, T. A. New nanocomposites for deep water deoxygenation. *Condensed Matter and Interphases*. 2021;23(43): 614–625. https://doi.org/10.17308/kcmf.2021.23/3682

31. Vakhnin D. D., Fertikova T. E., PolyanskiL. N., Kozaderov O. A., Kravchenko T. A. On the electrochemical deoxygenation of water with a nanocomposite containing copper metal nanoparticles and an ion-exchange polymer matrix. *Nanobiotechnology Reports*. 2022;17(6): 766–773. https://doi.org/10.1134/s2635167622060143

32. *Ion exchange resins. Cationites**. Specifications: GOST 0298-2022. Moscow: FGBU «RST»; 2022. 16 p. (in Russ.)

33. Kravchenko T. A., Kalinichev A. I., Polyansky L. N., Konev D. V. *Metal-ion exchanger nanocomposites**. Moscow: Nauka Publ.; 2009. 392 p. (in Russ.)

34. Damaskin B. B., Petriy O. A., Tsirlina G. A. *Electrochemistry: A Textbook**. 3rd ed., corrected. St. Petersburg: Lan' Publ.; 2021. 672 p. (in Russ.)

** Translated by author of the article*

Information about the authors

Dmitry D. Vakhnin, postgraduate student, Department of Physical Chemistry, Voronezh State University (Voronezh, Russian Federation).

vakhnin.dima@rambler.ru

Tatyana E. Fertikova, Cand. Sci. (Med.), Associate Professor, Department of General Hygiene, Voronezh State Medical University (Voronezh, Russian Federation).

https://orcid.org/0000-0002-4370-9197
tefertikova@vrngmu.ru

Natalya A. Zheltoukhova, master’s Student, Department of Physical Chemistry, Voronezh State University (Voronezh, Russian Federation).

zheltoukhova.natali@yandex.ru

Tamara Aleksandrovna Kravchenko, Dr. Sci. (Chem.), Full Professor, Department of Physical Chemistry, Voronezh State University (Voronezh, Russian Federation).

https://orcid.org/0000-0001-9214-7357
krav2809837@yandex.ru

Oleg Aleksandrovich Kozaderov, Dr. Sci. (Chem.), Associate Professor, Leading Researcher, Laboratory of organic additives for the processes of chemical and electrochemical deposition of metals and alloys used in the electronics industry, Voronezh State University (Voronezh, Russian Federation).

https://orcid.org/0000-0002-0249-9517
ok@chem.vsu.ru

Received January 28, 2025; approved after reviewing February 14, 2025; accepted for publication March 17, 2025; published online December 25, 2025.